Received: 28 October 2019 | Revised: 23 June 2020 | Accepted: 2 September 2020
DOI: 10.1002/2050-7038.12645

RESEARCH ARTICLE

WILEY

Applications of eigenvalues in installation of multi-infeed HVDC system for voltage stability

Bilawal Rehman[1,2] | **Chongru Liu**[1] | **Wei Wei**[3] | **Chuang Fu**[3] | **Huan Li**[3]

[1]State Key Laboratory of Alternate Electrical Power System with Renewable Energy Sources, North China Electric Power University, Beijing, China

[2]Department of Electrical Engineering, Knowledge Units of Engineering, University of Management & Technology, Sialkot, Pakistan

[3]State Key Laboratory of HVDC, Electric Power Research Institute, Guangzhou, China

Correspondence
Chongru Liu, State Key Laboratory of Alternate Electrical Power System with Renewable Energy Sources, North China Electric Power University, Changping District, Beijing 102206, China.
Email: chongru.liu@ncepu.edu.cn

Summary

This research work provides a practical approach to install High Voltage Direct Current (HVDC) link in close vicinity of an existing HVDC system. The work establishes eigenvalue-based approach using modal analysis to give voltage stability conditions for multi-infeed scenario. A detailed analysis of steady state and transient behavior of multi-infeed HVDC system is provided to understand the influence of network impedances. Minimum eigenvalue of AC-DC Jacobian matrix is taken as index to determine stability using a realistic multi-infeed HVDC model. Newton Raphson technique is applied to calculate bus angle and voltage for accurate stability analysis. The inter-converter interaction of multi-infeed HVDC severely affects the performance of AC/DC network. So, it is of great importance to study multi-infeed phenomena with a systematic way to minimize the risk of adverse results. Practical applications of proposed scheme are provided. It has been examined that the behavior of positive eigenvalue largely depends on coupling impedance while impedance between AC busbar and inverters show less control on region of stability. With increase in coupling impedance, multi-infeed interaction factor reduces which reflects less transient over voltage, commutation failure, and stability like problems. Various case studies are provided regarding network impedances to make system voltage stable. The results show that eigenvalues are greatly influenced by associated network impedances. The simulations are performed in MATLAB and PSCAD/EMTDC to verify the analytical results.

KEYWORDS

eigenvalues, HVDC installation, multi-infeed HVDC, voltage stability

List of symbols and abbreviations: CFII, commutation failure immunity index; EAC, grid voltage magnitude; ESCR, effective short circuit ratio; J_{11}, elements of Jacobian matrix; J_{12}, elements of Jacobian matrix; J_{21}, elements of Jacobian matrix; J_{22}, elements of Jacobian matrix; J_R, reduced Jacobian matrix; MIESCR, multi-infeed effective short circuit ratio; MIIF, multi-infeed interaction factor; ΔP, incremental change in active power; P_{dc}, DC power rating of HVDC; PBR, power base ratio; ΔQ, incremental change in reactive power; Q_c, available reactive power support of HVDC; ΔQ^{net}, net incremental change in power; ΔQ^{net}_{mi}, modal net power change; Q_{dc}, required reactive power support; SCR, short circuit ratio; T, transformer ratio; TOV, transient over voltage; $\Delta\delta$, incremental change in bus voltage angle; ΔV, incremental change in bus voltage magnitude; V_{dc}, voltage rating of HVDC; ΔV_{mi}, modal voltage change; X_T, transformer saturation reactance; Z_s, AC grid sources impedances; z_{12}, impedance between Bus 1-2; z_{13}, impedance between Bus 1-3; z_{23}, impedance between Bus 2-3; ξ, right eigenvector matrix; $\wedge$, diagonal eigenvalue matrix; η, left eigenvector matrix; λ, eigenvalue; γ, inverter extinction angle; α, rectifier firing angle; θ, AC grid voltage angle.

1 | INTRODUCTION

High Voltage Direct Current (HVDC) is evolving rapidly in modern power system transmission due to its significant advantages including bulk power transfer, control schemes, long distance, and operating modes.[1] With increased use of HVDC technology, situation arises where two or more HVDC links connect to AC systems which are in close electric proximity to meet load demand of area. This scheme of interconnection is termed as multi-infeed high voltage direct current transmission.[2] Such systems bring various concomitant operational challenges due to interaction between nearby HVDC links and AC system. Beside AC-DC interaction, the interaction between HVDC links of multi-infeed configuration degrades performance of converters.[3]

The behavior of steady state and transient phenomenon of multi-infeed DC systems is more challenging because of inter-converter interaction. The existing AC-DC interaction phenomena and related problems (such as commutation failure [CF], voltage stability, weak ac system, fault recovering time, and transient over voltage [TOV]) of single infeed DC system become more demanding in multi-infeed systems. Therefore, a quantitative and systematic mechanism for these multi-infeed phenomena is necessary to be established. Moreover, increasing challenges of multi-infeed DC systems demand an installation guide to provide an overall voltage stability.

Analysis of AC-DC power system stability has become a great concern of recent years. The stability of system voltage depends on AC system strength and load characteristics. Weak AC systems relative to power ratings of HVDC link are more susceptible to have voltage and power instability; and bring problems associated to power transfer and control. Since the inter-converter interaction affects the nearby ac system strength, so it significantly arises the stability issues.

Conventionally, effective short circuit ratio (ESCR) is being used as an index to evaluate voltage stability of system.[4] Higher value of ESCR reflects better voltage stability which is increased by various methods including synchronous compensator and condensers.[5] However, the ESCR is not valid for multi-infeed HVDC systems because of interaction between converters which negatively affects the performance. Multi-infeed effective short circuit ratio (MIESCR), an equivalent of ESCR, is proposed by CIGRE to quantitatively assess the AC system strength of multi-infeed DC systems considering nearby converters.[6] MIESCR incorporates multi-infeed interaction factor (MIIF) between converters during steady state conditions.[7] The MIESCR classify the voltage stability broadly without mentioning the specific parameters. Therefore, a detailed mechanism to investigate the voltage stability is required.

The maximum power curve (MPC) and voltage sensitivity factor (VSF) are two comprehensive approaches for voltage and power stability.[8] The maximum available power (MAP) based on MPC yields optimistic results for multi-infeed HVDC system due to interaction between inverters, which negatively influences the MAP. The MIIF not only influences the MAP but it also contributes in TOV, CF, and harmonics in AC-DC power system.[9]

Modal analysis is a mathematical technique that observes system stability based on VSF by evaluating eigenvalues of AC-DC power flow Jacobian matrix. The modal voltage sensitivity factor relates *V-Q* by eigenvalues. It is found to be an effective tool for system planners to identify practical solution of voltage instability. The MAP-based approach to evaluate voltage stability gives single degree of freedom (ie, DC current) while eigenvalue decomposition technique based on modal analysis gives more freedom to engineers to deal with system instability.[5]

In literature,[10] the voltage stability of multi-infeed DC systems is discussed considering a steady-state scenario which neglects dynamic behavior of electric load and AC system. Moreover, commutating AC buses are ignored while bus voltage and angle are considered static.[11] In Refs. 12 and 13, active power injection is assumed to be zero in order to simplify the equations but studies have shown that both active and reactive power influence the stability of system.[14] With these assumptions, the technique cannot be directly applied to practical projects.

In this work, angle and magnitude of commutating bus voltage along with real and reactive power for each converter are considered as state variables. The general equations are then formed in order to compute the stability of multi-infeed HVDC system. The role of network impedances (as in Figure 1) to bring system into stable region is also investigated for practical purposes. Here, the equivalent lumped parameters of transmission line are used as network impedances for simplicity.

The key objective of this study is to develop and investigate a general method based on eigenvalues to analyze voltage stability and associated problems in multi-infeed HVDC system. Reduced Jacobian with an additional active power based factor is used to compute eigenvalues of AC-DC network which can reflect any small change in state variables. It has been examined that the behavior of positive eigenvalue largely depends on coupling impedance while impedances between AC busbar and inverters show less control on region of stability. With increase in coupling impedance, multi-infeed interaction factor (MIIF) reduces which reflects less TOV, CF, and stability like problems. The impact of network

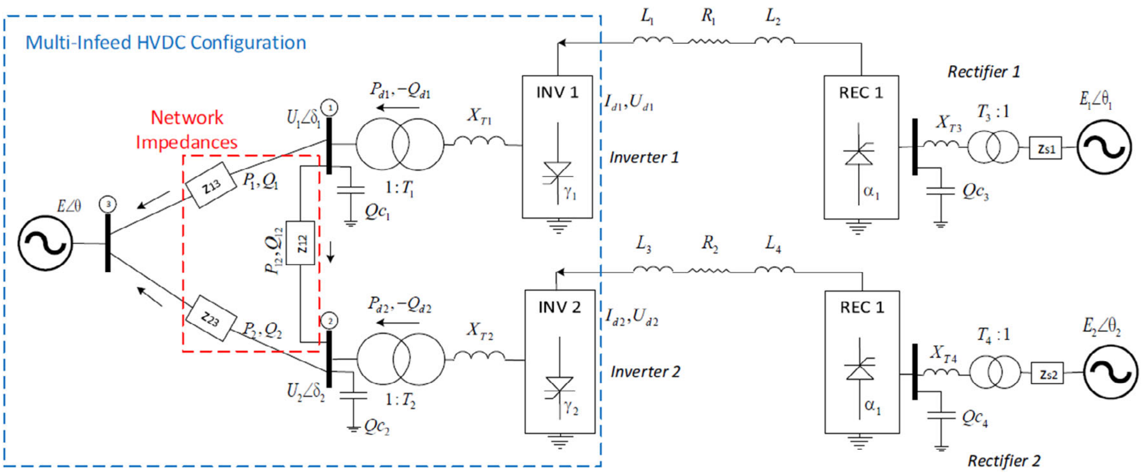

FIGURE 1 Multi-infeed HVDC topology

impedances is deeply investigated for MIIF, MIESCR, TOV, and CF immunity index (CFII). Practical realization of proposed scheme is also highlighted.

The converters under study are line commutated converters (LCC) which absorb huge reactive power consequently disturb system voltage stability. However, the method presented is independent of type of converters used. Therefore, the technique is valid for VSC-MMC and hybrid AC network.[15] In such cases, the elements of Jacobian matrix will change according to state variables.

The work is organized as follows: section 2 briefly describes modal analysis for voltage sensitivity. Mathematical equations are derived to incorporate active and reactive power in voltage stability. A relation to previously published work is also developed. Furthermore, the stability conditions are discussed and modal analysis for dual-infeed is also presented. Section 3 provides influence of network impedances on eigenvalues. Section 4 gives practical applications of proposed topology. Graphical results are presented in order to understand dual-infeed HVDC phenomena. Impact of network impedances on practical scenarios is also illustrated with minimum and maximum range. Discussion is provided in section 5 and conclusion is drawn in section 6.

2 | MODAL ANALYSIS

Modal analysis is an effective mathematical tool to evaluate stability of voltage. Pre modal analysis of power system can explain stability situations, which enable planners to estimate specification and parameters required in order to accomplish the overall stability of power system.[16] It is also well studied that modal analysis results are absolutely valid for any incremental change in system state variables.[13] For all buses, if bus V-Q sensitivity is positive, which means the bus voltage magnitude increases by ΔV with increase in reactive power injection ΔQ at same bus, then system is said to be voltage stable.[13] And a system is voltage unstable if V-Q sensitivity is negative for any bus. The power flow equations using Newton Raphson method can be written as Equation (1)

$$\begin{bmatrix} \Delta P \\ \Delta Q \end{bmatrix} = \begin{bmatrix} J_{11} & J_{12} \\ J_{21} & J_{22} \end{bmatrix} \begin{bmatrix} \Delta\delta \\ \Delta|V| \end{bmatrix} \tag{1}$$

ΔP and ΔQ are incremental real and reactive power, respectively. $\Delta\delta$ and $\Delta|V|$ are bus voltage angle and magnitude, respectively. While J_{11}, J_{12}, J_{21}, and J_{22} are elements of Jacobian matrix J. Solving Equation (1) for ΔQ results

$$\Delta Q = J_{21}J_{11}^{-1}\Delta P + \left(J_{22} - J_{21}J_{11}^{-1}J_{12}\right)\Delta V \tag{2}$$

To relate Equation (2) with previously published work,[10,13] reducing Equation (1) with $\Delta P = 0$ gives Equation (3)

$$\begin{cases} \Delta Q = J_R \Delta V \\ \Delta V = J_R^{-1} \Delta Q \end{cases} \tag{3}$$

Where $J_R = \left(J_{22} - J_{21} J_{11}^{-1} J_{12}\right)$

The Equation (2) can be rewritten in terms of reduced Jacobian matrix as Equation (4)

$$\Delta Q = J_{21} J_{11}^{-1} \Delta P + J_R \Delta V \tag{4}$$

Thus, Equation (4) explains that existing reduced Jacobian matrix-based techniques can also be employed to calculate V–Q sensitivity by incorporating ΔP. If the effect of ΔP is not neglected, ΔV would be Equation (5). It is to be noted that Equation (5) demonstrates analysis of system with reduced Jacobian plus an additional active power based factor; so it overall interprets effect of full Jacobian.

$$\Delta V = J_R^{-1} \left(\Delta Q - J_{21} J_{11}^{-1} \Delta P\right) \tag{5}$$

To draw analogy between Equations (3) and (5), we can introduce $\Delta Q^{net} = \left(\Delta Q - J_{21} J_{11}^{-1} \Delta P\right)$ so,

$$\Delta V = J_R^{-1} \Delta Q^{net} \tag{6}$$

Equation (6) gives a new relation to estimate stability by taking into account the effect of both real and reactive power. Modal decomposition of J_R^{-1} in Equation (6) results

$$J_R^{-1} = \xi \wedge^{-1} \eta \tag{7}$$

Assuming that ξ and η are right and left eigenvector matrix after normalization, whereas $\wedge$ is diagonal eigenvalue matrix of J_R. Equation (6) becomes

$$\begin{cases} \Delta V = \xi \wedge^{-1} \eta \Delta Q^{net} \\ \Delta V = \sum_i \frac{\xi_i \eta_i}{\lambda_i} \Delta Q^{net} \end{cases} \tag{8}$$

Where ξ_i and η_i denote i^{th} column right eigenvector and i^{th} row left eigenvector respectively.[13] Each value of λ_i with corresponding ξ_i and η_i represents i^{th} mode of response.[17] Since $\xi^{-1} = \eta$, Equation (8) reduces to Equation (9) which shows i^{th} modal voltage variation in response to net modal active and reactive power variation.

$$\Delta V_{mi} = \frac{1}{\lambda_i} \Delta Q_{mi}^{net} \because \begin{cases} \Delta V_{mi} = \eta_i \Delta V \\ \Delta Q_{mi}^{net} = \eta_i \Delta Q^{net} \end{cases} \tag{9}$$

Here, the $\eta_i \Delta V$ and $\eta_i \Delta Q^{net}$ are modal voltage and modal net reactive power variations respectively. Therefore,

$$\Delta Q_{mi}^{net} = \lambda_i \Delta V_{mi} \tag{10}$$

It is clearly seen that positive eigenvalues correspond to in phase modal voltage and modal reactive power relation indicating stable voltage. This means that incremental change in reactive power at bus cause increment in bus voltage. On other hand, if eigenvalues are negative; the system is voltage unstable, which means any incremental change in bus reactive power will cause bus voltage to decrease. If $|\lambda^{-1}| \to \infty$ or $|\lambda^{-1}| \to 0$, it means system is voltage unstable because any small change in net reactive power will reflect infinite change in bus voltage or any significant change in net reactive power will reflect a little change in bus voltage. Therefore, it reveals that magnitude of eigenvalues determines degree of voltage stability. This indicates that for stable voltage operation $|\lambda|$ should lie between 0 to a reasonable small number but not infinity.

2.1 | Dual infeed modal analysis

In this section, modal analysis of simplified dual infeed HVDC is briefly presented (Figure 1). The scheme under study is more realistic because both inverters are feeding into same AC bus. The most unstable and widely used control that is, constant gamma control mode is considered for analysis.[18] The converters in multi-infeed system are taken as load instead of source to network by inverting signs of real and reactive power. This simplifies the network but does not affect the results. Buses 1 and 2 are *P–Q* buses, while bus 3 is taken as slack bus for Newton Raphson analysis.

The elements of Equation (1) for dual infeed are.

$$\Delta P = \begin{bmatrix} \Delta P_1 \\ \Delta P_2 \end{bmatrix}, \Delta Q = \begin{bmatrix} \Delta Q_1 \\ \Delta Q_2 \end{bmatrix}, \Delta\delta = \begin{bmatrix} \Delta\delta_1 \\ \Delta\delta_2 \end{bmatrix}$$

and $\Delta|V| = \begin{bmatrix} \Delta|V_1| \\ \Delta|V_2| \end{bmatrix}$

While elements of Jacobian matrix are.

$$J_{11} = \begin{bmatrix} \frac{\partial P_1}{\partial \delta_1} & \frac{\partial P_1}{\partial \delta_2} \\ \frac{\partial P_2}{\partial \delta_1} & \frac{\partial P_2}{\partial \delta_2} \end{bmatrix}, J_{12} = \begin{bmatrix} \frac{\partial P_1}{\partial |V_1|} & \frac{\partial P_1}{\partial |V_2|} \\ \frac{\partial P_2}{\partial |V_1|} & \frac{\partial P_2}{\partial |V_2|} \end{bmatrix} \; J_{21} = \begin{bmatrix} \frac{\partial Q_1}{\partial \delta_1} & \frac{\partial Q_1}{\partial \delta_2} \\ \frac{\partial Q_2}{\partial \delta_1} & \frac{\partial Q_2}{\partial \delta_2} \end{bmatrix}, J_{22} = \begin{bmatrix} \frac{\partial Q_1}{\partial |V_1|} & \frac{\partial Q_1}{\partial |V_2|} \\ \frac{\partial Q_2}{\partial |V_1|} & \frac{\partial Q_2}{\partial |V_2|} \end{bmatrix}$$

The dual infeed *V-Q* sensitivity relation, using Equation (10), becomes,

$$\begin{bmatrix} \Delta Q_1 \\ \Delta Q_2 \end{bmatrix}^{net} = \lambda_{\min} \begin{bmatrix} \Delta V_1 \\ \Delta V_2 \end{bmatrix} \tag{11}$$

For overall stability of dual infeed HVDC system, slope of *V-Q* sensitivity must be positive with minimum positive eigenvalue.

The steady state and transient phenomena related to multi-infeed HVDC are briefly discussed in Table A1. However, the reader is referred to[6,19-22] for more details.

3 | INFLUENCE OF NETWORK IMPEDANCES

The elements of Jacobian matrix are function of network impedances z_{12}, z_{13}, and z_{23}; so eigenvalues of Jacobian matrix are also function of these impedances. This implies that variation in any of impedance directly affects stability. Equation (11) reveals that for positive *V–Q* sensitivity, all eigenvalues of Jacobian matrix must be positive. Therefore, the network impedances are chosen in such a way that $\lambda_{min} > 0$ which result in $\det(J) > 0$. This section analyzes the influence of network impedances on eigenvalues of system.

The z_{13} is attached between buses 1 and 3. The z_{13} is actually the equivalent impedance of lumped parameters of small transmission line between converter 1 and receiving end power system (bus 3). The behavior of minimum eigenvalue vs z_{13} is shown in Figure 2(A) for $PBR < 1$ and constant z_{12} and z_{23}. The $PBR < 1$ means that HVDC 1 has higher power rating relative to HVDC 2. It can be seen that system shows transition between stable and unstable region with lower value of z_{13}; however, system moves to stable region with increase in z_{13}. It can also be seen that as coupling impedance (z_{12}) increases, the system moves very fast to region of positive eigenvalues but for short span of z_{13}. This indicates that z_{13} has less control on stability or provides less flexibility in order to control the eigenvalues; and with further increase in z_{13} system moves to unstable region. This means, the system planners need to choose z_{13} from a small range of values. The z_{13} also offers less control on ESCR in stable region. If the PBR approaches to 1 then the range of z_{13} for voltage stability reduces.

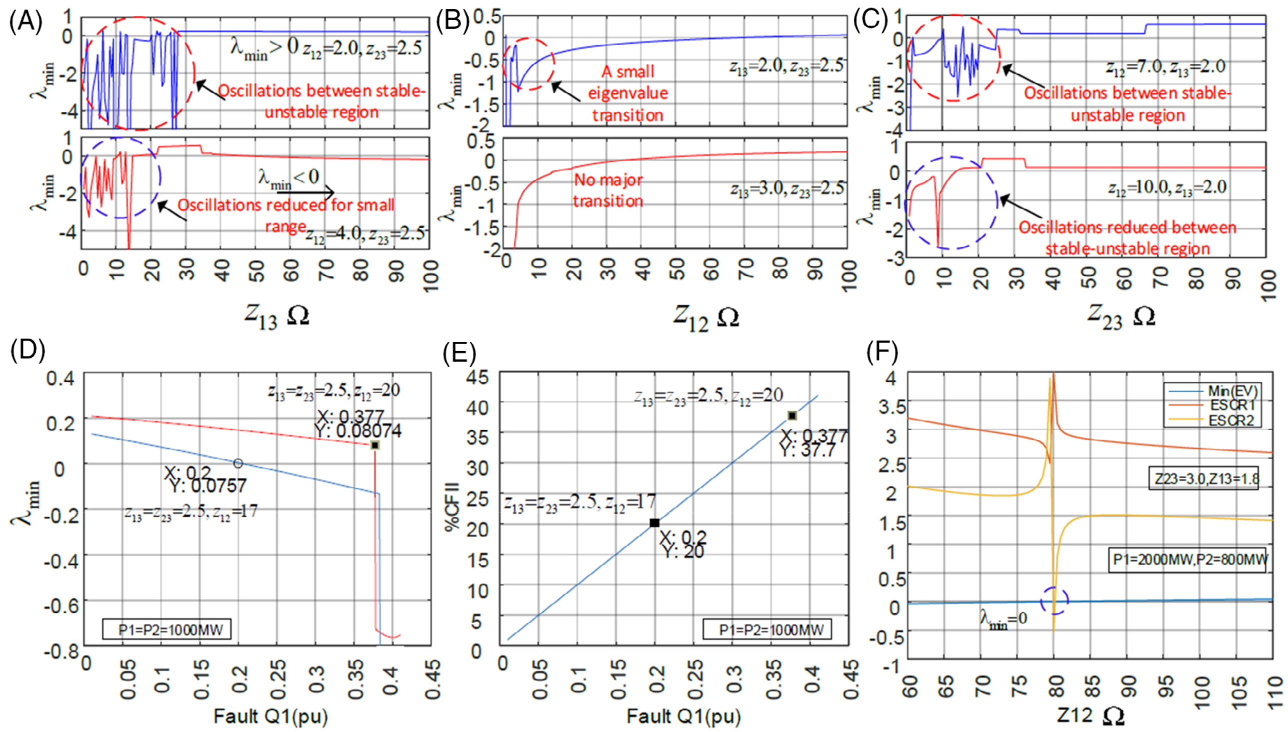

FIGURE 2 Impact of network impedances on eigenvalues **(**A) λ_{min} vs z_{13} (B) λ_{min} vs z_{12} (C) λ_{min} vs z_{23} (D) λ_{min} vs Fault Q (E) CFII vs Fault Q (F) ESCR and λ_{min} vs z_{12}

The electrical network between HVDC converters is simplified as tie line having equivalent impedance of z_{12}, which shows the closeness between the converters of multi-infeed HVDC configuration. The coupling impedance (z_{12}) is attached between bus 1&2 of converter 1 and converter 2, respectively. The influence of z_{12} on λ_{min} of system with constant z_{13} and z_{23} is shown in Figure 2(B). The graph shows that minimum eigenvalue moves very fast to stable region with increase in coupling impedance. It is also examined that increase in z_{13} and z_{23} does not result any kind of system oscillations between stable and unstable region but provide a new range of impedances for positive λ_{min}. Moreover, the system remains in stable region of operation with even higher values of $z_{12,}$ which describes its large control on stability. This provides a freedom to designers to set z_{13} and z_{23} and then choose z_{12} among the large range of values. The response of ESCR and λ_{min} with z_{12} is presented in Figure 2(F). ESCR shows spikes with $\lambda_{min} = 0$ which expounds the sudden increase in bus voltage as described in section 2 because of singularity of Jacobian matrix.

The z_{23} is attached between buses 2 and 3. The z_{23} is actually the equivalent impedance of lumped parameters of small transmission line between converter 2 and receiving end power system (bus 3). The effect of increasing z_{23} on minimum eigenvalue is illustrated in Figure 2C for constant z_{12} and z_{13} and $PBR < 1$. It can be observed that the transition between stable and unstable regions reduces as z_{23} increases and higher z_{12} requires less z_{23} for stable region. On other hand, the system remains in stable region with increase in $z_{23,}$ which corresponds to provide wide range of z_{23} to make system stable but significant increase in z_{12} makes system oscillating between positive and negative eigenvalue. This implies that z_{23} has much more control on eigenvalues than z_{13} with $PBR < 1$ and as minimum eigenvalue approaches to zero, the system voltage collapse and ESCR reflects spikes due to TOV. It is worth mentioning that role of z_{13} and z_{23} will be reversed with $PBR > 1$.

The coupling impedance not only plays role in stability but it also affects transient phenomena. The topology under study (Figure 1) reflects higher ESCR than single infeed due to influence of network impedances. MIESCR, MIIF, TOV, CFII, and ESCR are also dependent on network impedances which reflects significant control of network impedances on stability related phenomena.

As $z_{12} \rightarrow \infty$, $MIIF \rightarrow 0$ means that influence of nearby converter *j* on voltage of converter *i* is negligible or zero which physically explains that both inverters are electrically isolated (Figure 7). And this is the best phenomenon one would expect. Less MIIF reduces TOV, CF, and stability related problems. HVDC with relatively large in power influences more to nearby converters; which authenticates the CIGRE comments on multi-infeed HVDC. It is investigated that high value of coupling impedance reduces TOV effect (Figure 8) and slightly increase ESCR. System ESCR reduces with increase in TOV, which also authenticates the CIGRE claim. It is also found that high power rating link will severely affect nearby link during TOV situation.

CF brings significant voltage dip at converter bus, which moves system to unstable region of operation with negative eigenvalues. The CFII is also correlated with z_{12}; higher the value of z_{12} is the more time system will take to move to unstable region. Figure 2(D and E) represent minimum eigenvalue and CFII, respectively. It can be realized that higher coupling impedance yields more CFII.

4 | APPLICATIONS

In this section, practical realization of impact of network impedances on stability with proposed topology is discussed. As eigenvalue (λ_{min}) of network Jacobian directly depends on z_{12}, $z_{13,}$ and z_{23}. So, there are variety of graphs to explain system behavior but our concern is with only minimum eigenvalue. The dependency of λ_{min} on network impedances implies to indirectly dependency on MIESCR and *PBR* of dual-infeed HVDC converters. Nominal DC power and AC voltage of inverter 1 are taken as base power and base voltage, respectively. All units are properly mentioned on each graph.

4.1 | Installation of new HVDC link

A HVDC link 1 of 1000 MW, 500 kV is working in stable region. A new HVDC link 2 of 600 MW, 500 kV is supposed to be installed on same AC busbar (Figure 3). In this scenario 1, the designers would be interested to know the limitations in voltage stability of overall system. Thus, for voltage stability, the z_{12} and z_{23} need to be calculated with parameters of existing and newly installed HVDC links for $\lambda_{min} > 0$. The $z_{13} = 2.5$ for voltage stable operation of HVDC 1.

A few values of network impedances for voltage stable operation are presented in Table 1. Figure 4 shows λ_{min} vs z_{12}; stable and unstable region is also marked.

4.2 | To bring existing system into stable region

Another important application is to bring existing unstable HVDC 1 (suppose 2000 MW, 500 kV) into stable region of operation with the help of newly installed HVDC 2 (suppose 800 MW, 500 kV) and network impedances. In this scenario 2, z_{12} and z_{23} should be calculated which would reflect $\lambda_{min} > 0$ with existing unstable and newly installed HVDC links parameters. Here, $z_{13} = 1.8$ is chosen which would result unstable HVDC 1 voltage. Values of network impedances with constant z_{13} are listed in Table 2 for overall stable operation.

Variation of λ_{min} vs z_{12} is depicted in Figure 5 for two values of z_{23}.

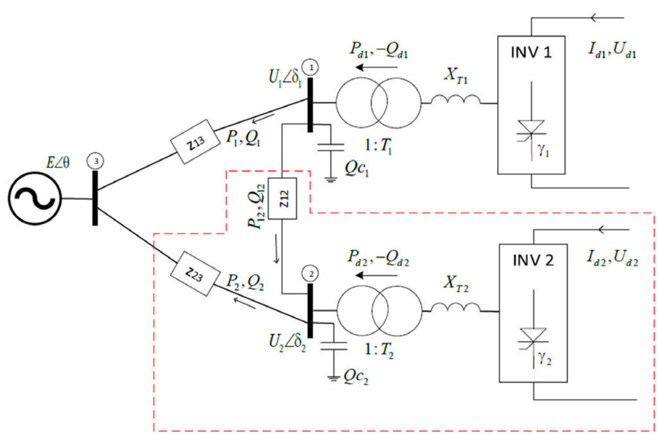

FIGURE 3 Scenarios 1 and 2 (HVDC 1 is considered stable and unstable, respectively)

P_{dc1}	V_1	P_{dc2}	V_2	z_{12} (Ω)	z_{13} (Ω)	z_{23} (Ω)
1000(MW)	500(kV)	600(MW)	500(kV)	>20	>2.1	3.5
				>28	2.5	2.1
				>35	2.5	2.0
				>49.5	2.5	1.9

TABLE 1 Values of z_{12}, z_{13} and z_{23} for voltage stability

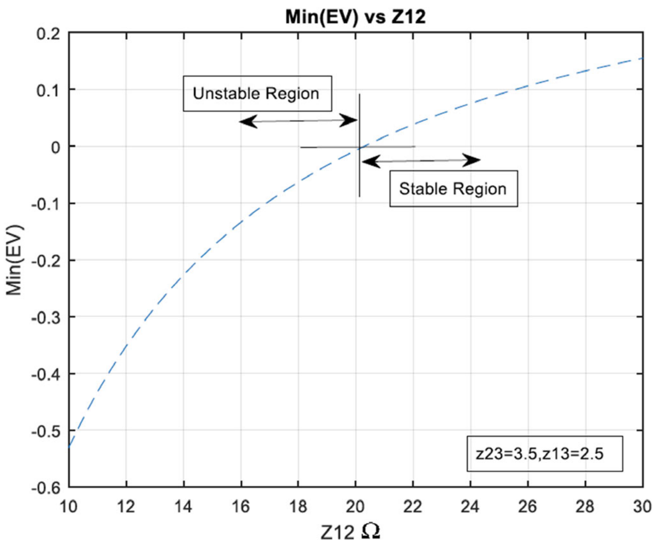

FIGURE 4 Scenario 1, λ_{min} vs z_{12}

The phenomena MIIF, TOV, CFII, ESCR, and MIESCR are presented only for scenario 2 due to space limitation of paper.

The inter-converter influence of converters in close proximity affects the ESCR; converter with large power rating reduces ESCR while converter of low power rating increases ESCR due to influence of MIIF (Figure 6). Thus, MIESCR is found to be an accurate index to determine system strength.

Figure 7 shows behavior of MIIF vs z_{12}; $\Delta Q = 0.01$ (p.u.) is injected at bus 1 and 2 for $MIIF_{21}$ and $MIIF_{12}$, respectively. It can be seen that inverter 1 of 2000 MW influence more to inverter 2 with 800 MW which authenticates CIGRE comments on multi-infeed. Moreover, it is evident that MIIF reduces with higher values of coupling impedance.

Figure 8 explains TOV vs z_{12}; $\Delta Q = 0.6$ (p.u.) is taken for worst case situation at bus 1. As shown in Figure 2(F), $\lambda_{min} = 0$ gives sudden rise in bus voltage (discussed in section 2).

Figure 9 shows variation of TOV vs Q_{inj}. Keeping all network impedances as constant, system shows transition to unstable region of operation with huge reactive power injection ($Q_{inj} > 0.19$ (p.u.)) at bus 1 which results negative eigenvalue at around 32% TOV.

To calculate CFII, a fault having reactive power of Q_f is applied at commutation bus and extinction angle is observed. The extinction angle less than 8° denotes a CF. The value corresponding to maximum Q_f without voltage collapse is CFII (19%), discussed in Appendix A, as indicated in Figure 10.

P_{dc1}	V_1	P_{dc2}	V_2	z_{12}(Ω)	z_{13}(Ω)	z_{23}(Ω)
2000(MW)	500(kV)	800(MW)	500(kV)	>134	1.8	2.9
				>80	1.8	3.0
				>61.6	1.8	3.1
				>53.5	1.8	3.2

TABLE 2 Values of z_{12}, z_{13} and z_{23} for voltage stability

FIGURE 5 Scenario 2, λ_{min} vs z_{12}

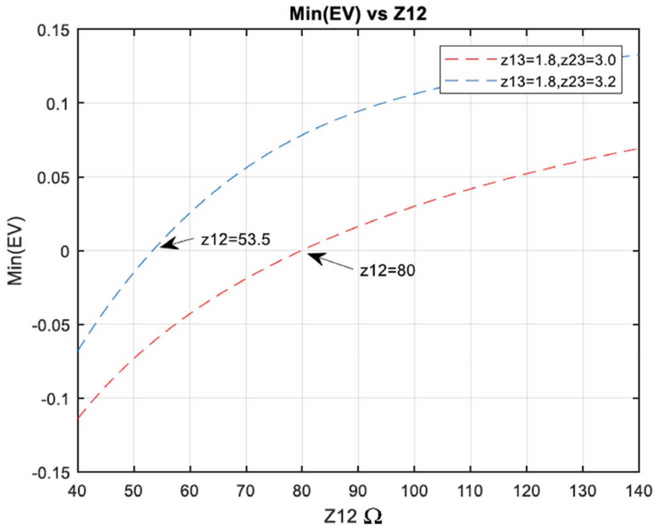

FIGURE 6 Behavior of $ESCR_{1,2}$, MIIF and MIESCR vs z_{12}

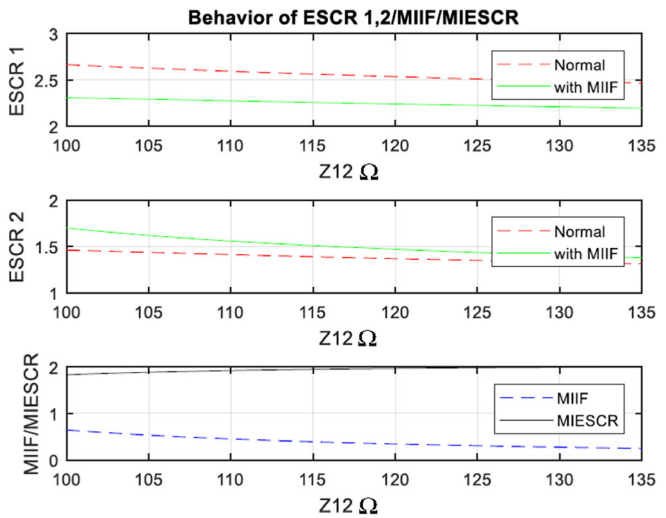

FIGURE 7 Behavior of MIIF vs z_{12}

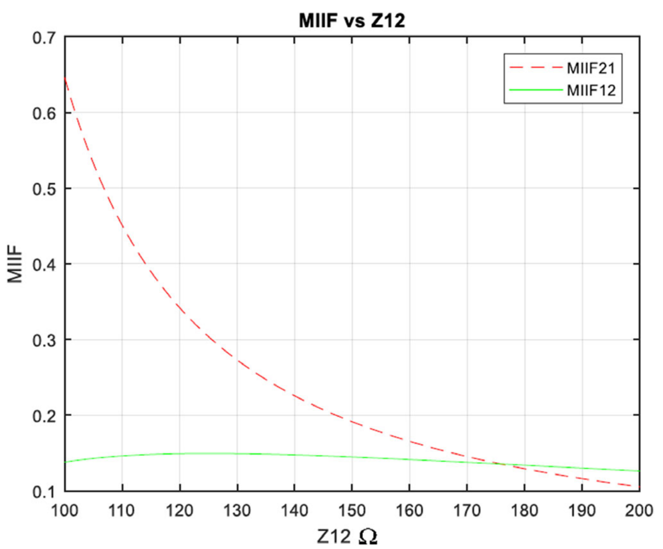

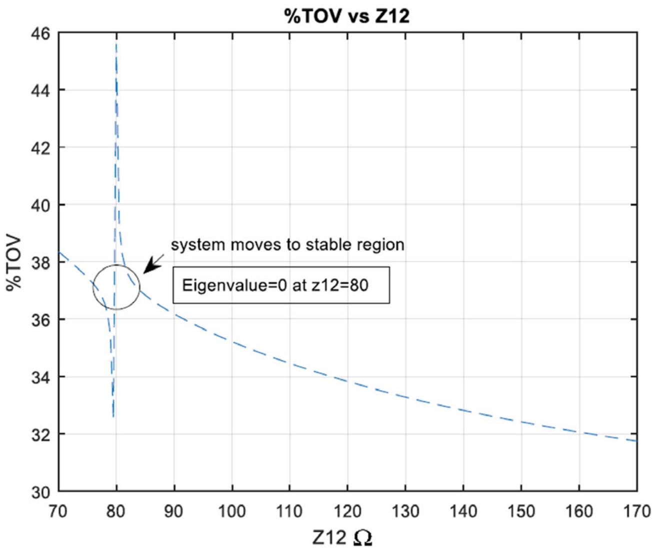

FIGURE 8 TOV vs z_{12}

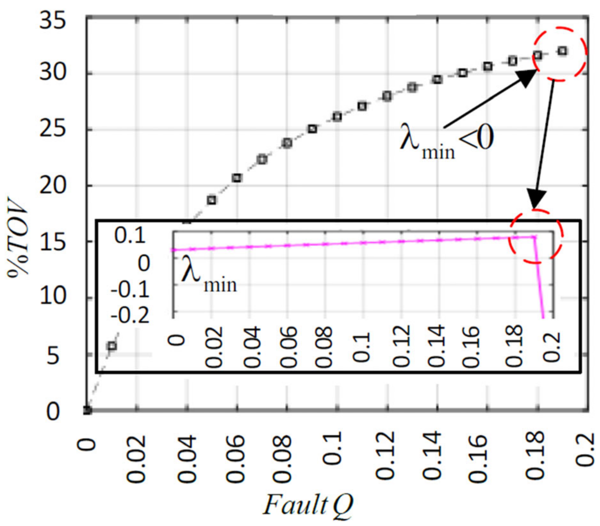

FIGURE 9 TOV vs Q_{inj} and λ_{min} vs Q_{inj}

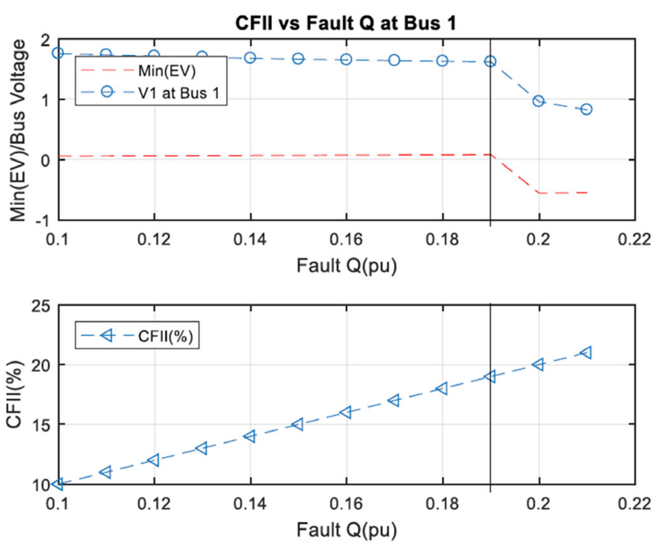

FIGURE 10 CFII vs Fault Q

4.3 | Application to single-infeed HVDC

One of the most important applications of proposed topology is to make single infeed HVDC system stable with the help of network impedances and voltage source (Figure 11). Suppose we have 1000 MW, 500 kV single infeed HVDC system with only $z_{13} = 1.5$. To make system voltage stable, designers need to calculate z_{12} and z_{23} with existing HVDC parameters and a voltage source $V_2\angle\delta_2$ which produce $\lambda_{min} > 0$. Here, the voltage source means a practical voltage source having some impedance.

It is observed that single infeed HVDC system should have $z_{13} > 1.2$ in order to make it stable with given topology. The λ_{min} w.r.t. z_{12} is shown in Figure 12. Table 3 gives comprehensive data for voltage stable conditions.

4.4 | PSCAD/EMTDC simulations

To validate proposed topology, a dual infeed LCC HVDC system with HVDC links of rating 1000 MW, 500 kV each is modeled in PSCAD/EMTDC. Schematic diagram of Figure 1 is given in Figure 13. Here, transformer as impedance device is used between all buses. Two sets of analytical results for stability of system under study are given in Table 4.

Figure 14 shows stable/unstable RMS AC voltage with $SCR = 2.5$. The simulation results are clear and self-explanatory in terms of stability. Table 4 and Figure 14 are coherent to each other.

As weak AC system results more instability than strong, so a comparison with various *SCR(s)* is also illustrated in Figure 15. It is evident that strong AC system exhibits less oscillations during instability; however, a weak system is

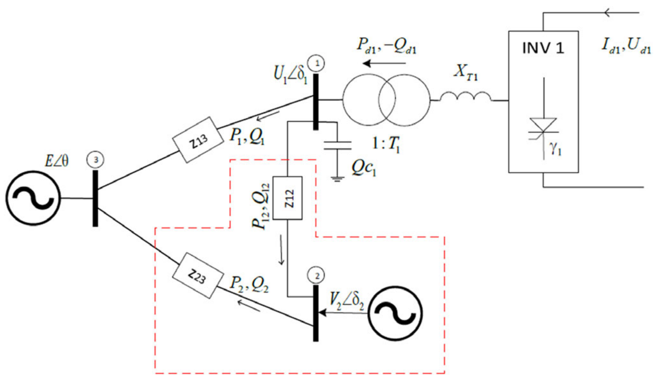

FIGURE 11 Application to single infeed HVDC

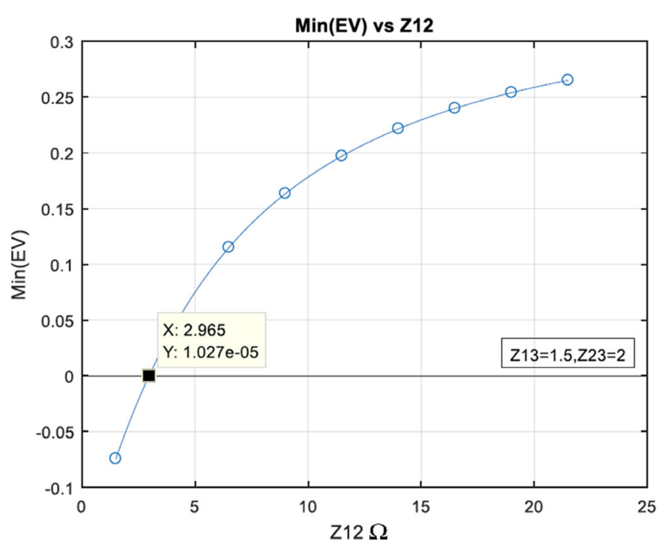

FIGURE 12 λ_{min} vs z_{12}

$z_{13}(\Omega)$	$z_{12}(\Omega)$	$z_{23}(\Omega)$	V_2(p.u.)	δ_2(rad)
1.3	>2.275	1	1.5	1.5
1.3	>3.935	1.5	1.5	1.5
1.3	>5.160	2	1.5	1.5
1.5	>1.510	1	1.5	1.5
1.5	>2.385	1.5	1.5	1.5
1.5	>2.965	2	1.5	1.5
1.5	>5.10	2	1	1.5
1.5	>4.505	1.5	1	1.5
1.5	>8.385	1.5	0.5	1.5
1.5	>5.100	2	1.0	1.5
2	>2.870	2	1.0	1.5
2.1	>2.705	2	1.0	1.5
2.4	>2.365	2	1.0	1.5

TABLE 3 Values of z_{12}, z_{13} and z_{23} for voltage stability

affected more because of unstable voltage fluctuations. Practically, the strength of AC system can be improved by installing reactive power compensators at commutating bus, which results less source impedance.

To analyze the impact of coupling impedance, a weak system with SCR of 2.0 is observed under increased coupling impedance and results are shown in Figure 16. The results are quite satisfactory that with higher value of z_{12} the system shows less magnitude of unstable voltage. This validates the analytical observation that higher value of coupling

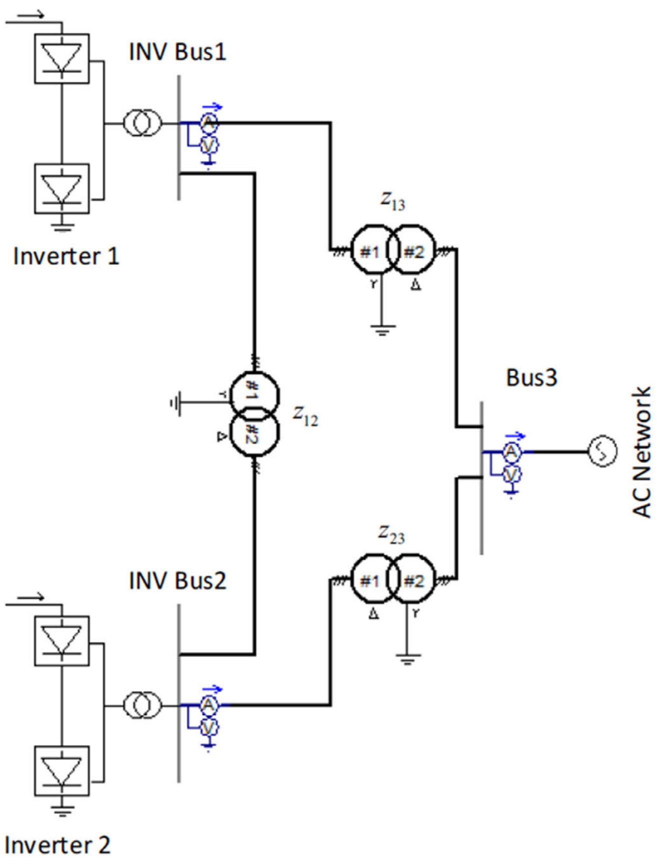

FIGURE 13 Schematic diagram of dual infeed LCC HVDC

TABLE 4 Dual infeed LCC HVDC stability conditions

$P_{dc1} = P_{dc2}$	$V_1 = V_2$	$z_{13}(\Omega)$	$z_{12}(\Omega)$	$z_{23}(\Omega)$
1000 MW	500 kV	2.5	>37.75	2.0
		2.5	>15.3	2.5

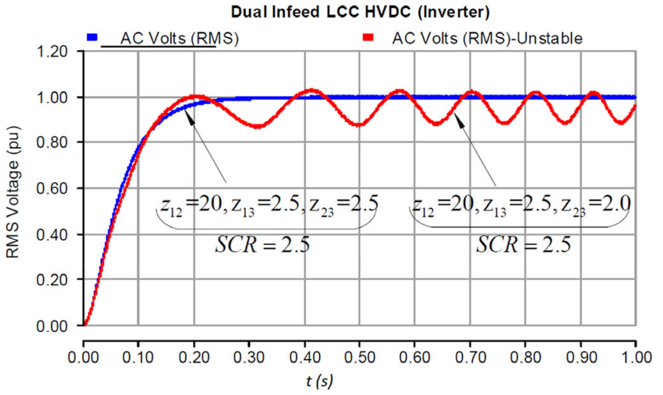

FIGURE 14 Stable (blue) and unstable (red) scenarios

impedance gives more stability and eventually increases MIESCR (Figure 8), reduces MIIF (Figure 3), reduces TOV (Figure 4) and increases CFII (Figure 2(E)).

Figure 17 shows response of voltage magnitude under stable/unstable conditions after a small disturbance produced by switching a capacitor and inductor at AC bus. The *SCR* and network impedances are mentioned on the graph. It is clear from the graph that reactive power variation reflects positive *V*–*Q* sensitivity and this is the most appropriate condition required for stability achieved by proposed model.

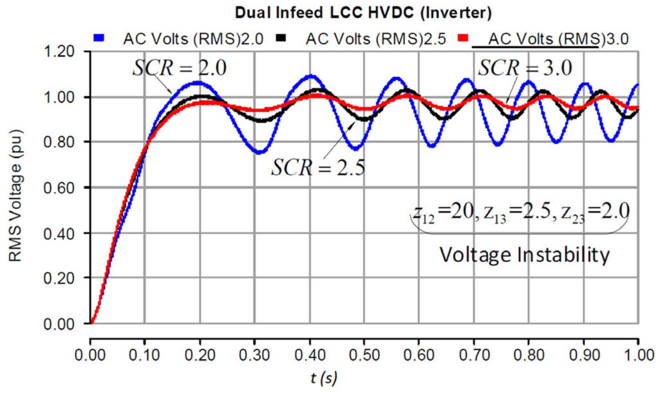

FIGURE 15 Voltage stability comparison with different SCR values

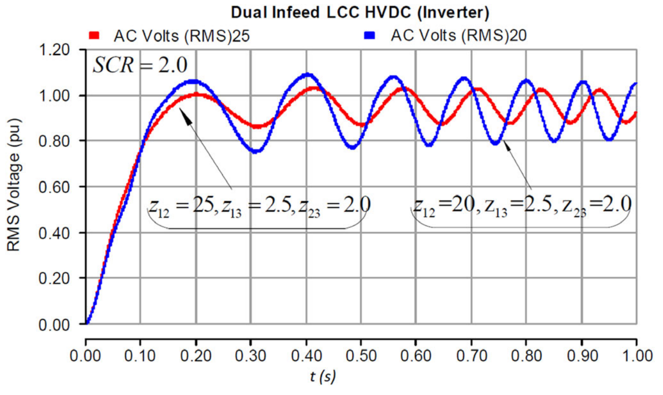

FIGURE 16 Influence of z_{12} on unstable voltage magnitude

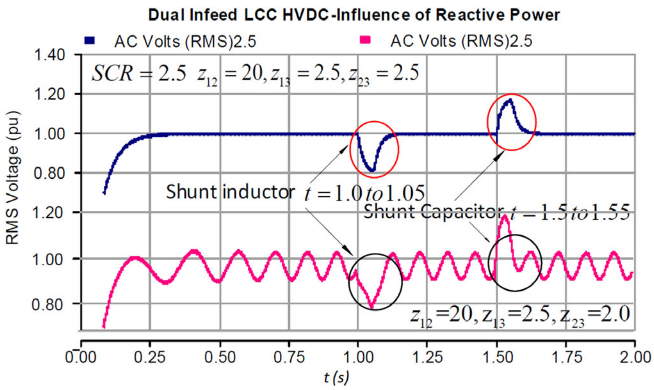

FIGURE 17 Reactive power impact during stable (blue) and unstable scenario (red)

5 | DISCUSSION

An eigenvalues-based approach to analyze the voltage stability of multi-infeed HVDC is presented. A power flow approach is applied to calculate the state variables of the system. It is investigated that the voltage stability of multi-infeed HVDC system depends on eigenvalues of AC/DC Jacobian matrix; and the eigenvalues of system vary with network impedances attached between commutating buses and receiving end AC system. The role of these network impedances is described in detail where it is clear that coupling impedance between two inverters influences the stability more as compared to other impedances.

It is analyzed that the coupling impedance (z_{12}) also plays role in steady state and transient phenomena. As z_{12} increases, the MIIF reduces which increases MIESCR and concurrent CFII. Thus, the network impedances associated with multi-infeed HVDC not only affect the stability but these also reduce the worst transient phenomena. The practical applications show the applicability of technique presented. The technique discussed is highly usable in future where several HVDC links not only lie in close proximity but on same busbar. The distinct feature of proposed technique is the use of voltage source to make existing single infeed stable (Figure 11). The analytical results of MATLAB are verified in PSCAD/EMTDC software.

6 | CONCLUSION

In this research work, a general method to analyze the stability of multi-infeed HVDC system using eigenvalue decomposition technique is presented. A realistic model of multi-infeed HVDC is used for stability analysis in which both inverters are feeding into same AC busbar. The analysis presented uses eigenvalues of reduced Jacobian with an additional active power based factor, which consequently incorporates active and reactive power variation at bus to determine voltage stability. Bus voltage and angle are calculated using Newton Raphson technique for accurate results. It is found that eigenvalues largely depend on network impedances z_{12}, z_{13} and z_{23}. Higher value of coupling impedance (z_{12}) reduces MIIF and TOV and increases local CFII. As $z_{12} \rightarrow \infty$, $MIIF \rightarrow 0$, which means both inverters are isolated and operating as single infeed. Converters with large power rating will influence more to converters with small power rating in normal and TOV conditions. It is also observed that with the help of network impedances ESCR of single infeed HVDC improves. A few practical applications of proposed topology are also discussed. It is illustrated that given topology can reveal voltage stability conditions of multi-infeed and suggest practical parameters to make it stable if the system is working in unstable region. A scheme to make single infeed HVDC system stable with the help of network impedances is also discussed. The analytical results are verified using PSCAD/EMTDC simulation tool. The graphical behavior of simulated results is closely related to analytical calculations.

Practical realization of eigenvalues is explored in installation of new HVDC link in close proximity of existing HVDC link. The analysis presented in this article can be used as technical guide for practical projects.

ACKNOWLEDGEMENTS

The authors acknowledge the financial support from Science and Technology project of Southern Power Grid of China under Grant ZBKJXM20180104.

PEER REVIEW

The peer review history for this article is available at https://publons.com/publon/10.1002/2050-7038.12645.

DATA AVAILABILITY

The data related to findings of this article are available from first author (BR) upon reasonable request.

ORCID

Bilawal Rehman https://orcid.org/0000-0002-7007-5679

REFERENCES

1. Rehman B, Liu C. A generalized N terminal current order control scheme for LCC MTDC. Paper presented at: IEEE 2nd International Electrical and Energy Conference (CIEEC); November 4-6,2018; Beijing, China. 344–349.
2. Rehman B, Liu CAC. DC multi-infeed power flow solution. *IET Gener Transm Distrib*. 2019;13(10):1838-1844. https://doi.org/10.1049/iet-2018.6781.
3. Wang L, Yang ZH, Lu XY, Prokhorov AV. Stability analysis of a hybrid multi-infeed HVDC system connected between two offshore wind farms and two power grids. *IEEE Trans Ind Appl*. 2017;53(3):1824-1833.
4. Ni X, Gole AM, Zhao C, Guo C. An improved measure of AC System strength for performance analysis of multi-infeed HVdc systems including VSC and LCC converters. *IEEE Trans Power Deliv*. 2018;33(1):169-178.
5. Zhang X, Chen C. Maximum available power of multi-infeed hvdc system analysed by sensitivity method. *IET Gener Transm Distrib*. 2014;8(3):473-479.
6. B. Davies, A. Williamson, A. M. Gole, et al. Systems with multiple DC infeed. *Cigré* (Publication 364) 2008:1-118. (WG B4.41).
7. Toledo PF, Bergdahl B, Asplund G. Multiple infeed short circuit ratio—aspects related to multiple HVDC into one AC network. *IEEE/PES Transm Distrib Conf Expo Asia Pac*. 2005;1-6. https://doi.org/10.1109/TDC.2005.1546774.
8. Lee D, Aik H, Anderson G. Power stability analysis of multi-infeed HVDC systems. *IEEE Trans Power Deliv*. 1998;13(3):923-931.
9. Chen X, Gole AM, Han M. Analysis of mixed inverter/rectifier multi-infeed HVDC systems. *IEEE Trans Power Deliv*. 2012;27(3):1565-1573.
10. Lee D, Aik H, Anderson G. Voltage stability analysis of multi-infeed HVDC systems. *IEEE Trans Power Deliv*. 1997;12(3):1309-1318.
11. Lee DHA, Andersson G. An equivalent single-infeed model of multi-infeed HVDC systems for voltage and power stability analysis. *IEEE Trans Power Deliv*. 2016;31(1):303-312.
12. Aik DLH. Voltage stability assessment using equivalent nodal analysis. *IEEE Trans Power Syst*. 2016;31(1):454-463.
13. Gao B, Morison GKGK, Kundur P. Voltage stability evaluation using modal analysis. *IEEE Trans Power Syst*. 1992;7(4):1529-1542. https://doi.org/10.1109/59.207377.
14. Wu G, Minakawa T, Hayashi T. Modal voltage stability analysis of multi-infeed HVDC System considering its control systems. *IEEJ Trans Power Energy*. 2006;126(8):776-782. https://doi.org/10.1541/ieejpes.126.776.
15. Aik DLH, Andersson G. Analysis of voltage and power interactions in multi-infeed HVDC systems. *IEEE Trans Power Deliv.* 2013;28(2):816-824.
16. Pinto HJCP, Martins N, F XV, Bianco A, Gomes P, Santos MGD. Modal analysis for voltage stability: application at base case and point of collapse. *Bulk Power System Voltage Phenomena - III Voltage Stability, Security & Control*. Fairvax, Va: ECC; 1994:1-14.
17. Kundur P, Rogers GJ, Wong DY, Eigenvectors E, Response F, System P. A comprehensive computer program package for small signal stability analysis of power systems. *IEEE Trans Power Syst*. 1990;5(4):1076-1083.
18. Zheng A, Guo C, Cui P, Jiang W, Zhao C. Comparative study on small-signal stability of LCC-HVDC system with different control strategies at the inverter station. *IEEE Access*. 2019;7:34946-34953.
19. Kundur P. *Power System Stability and Control*. EPRI Power System Engineering Series. McGraw-Hill; 1994.
20. Davies JB. Systems with multiple DC infeed. *Cigre WG*. 2007;B441:1-6. https://doi.org/10.1016/j.ijindorg.2010.06.004.
21. Rahimi E. *Voltage Interactions and Commutation Failure Phenomena in Multi-Infeed HVDC Systems, University of Manitoba*. Department of Electrical and Computer Engineering; 2011.
22. Rahimi E, Gole AM, Davies JB, Fernando IT, Kent KL. Commutation failure analysis in multi-infeed HVDC systems. *IEEE Trans Power Deliv*. 2011;26(1):378-384. https://doi.org/10.1109/TPWRD.2010.2081692.

How to cite this article: Rehman B, Liu C, Wei W, Fu C, Li H. Applications of eigenvalues in installation of multi-infeed HVDC system for voltage stability. *Int Trans Electr Energ Syst*. 2020;e12645. https://doi.org/10.1002/2050-7038.12645

APPENDIX: A1. Appendix

SCR and ESCR: AC system strength is measured with short circuit ratio (SCR) and effective short circuit ratio (ESCR). In fact, these two are correlated. Although, these are not a full measure of system various phenomena but still these are effective tool to judge system strength broadly. SCR is defined as Equation (A1) but it is more convenient to describe system strength including AC side installed equipments as ESCR in Equation (A2). The Qc_i is total MVA of capacitors and AC filters installed at converter bus i

$$SCR_i = \frac{\text{short circuit MVA}(\text{AC system})_i}{\text{rated MW}(\text{converter})_i} = \frac{V_i^2/z_i^{th}}{Pdc_i} \tag{A1}$$

$$ESCR_i = \frac{\left(V_i^2/z_i^{th}\right) - Qc_i}{Pdc_i} \tag{A2}$$

PBR: Power base ratio (PBR) is an important term in multi-infeed HVDC system, which describes relative converter power ratings, defined as Equation (A3). It helps to normalize both inverters on single base.

$$PBR = \frac{Pdc_2}{Pdc_1} \tag{A3}$$

Nominal DC power and AC voltage of inverter 1 are taken as base power and base voltage respectively. Thus,

$$ESCR_2 = \frac{1}{PBR}\left(ESCR_2^*\right)$$

Here, $ESCR_2^*$ denotes effective SCR with base values of inverter 2.

MIIF: Multi-infeed interaction factor (MIIF) is a quantitative index, which explains level of voltage interaction between converters in close electric proximity. MIIF is a ratio of incremental change in bus i voltages to incremental change in bus j voltages caused by any incremental injection of reactive power at bus j. The $\Delta V_j = 1\%$ of rated voltages is recommend. MIIF ranges from 0 to 1 which tells degree of closeness between two HVDC converters. The 0 means both buses are infinitely far away and do not have impact on each other. While 1 implies that both converters are attached to same bus with 100% interaction.

$$MIIF_{i,j} = \frac{\Delta V_i}{\Delta V_j} \tag{A4}$$

It is found that if $MIIF < 0.15$ then chances of voltage interaction is small. However, $0.15 \le MIIF < 0.40$ indicates moderate chances of interaction and $MIIF \ge 0.40$ corresponds high voltage interaction.

MIESCR: Multi-infeed effective short circuit ratio (MIESCR) is analogous to ESCR in single infeed HVDC. MIESCR explains the influence of nearby converter on the strength of system. It can be defined as Equation (A5). Here, j denotes all links in close proximity.

$$MIESCR_i = \frac{\left(V_i^2/z_i^{th}\right) - Qc_i}{Pdc_i + \sum_j MIIF_{ji} \times Pdc_j} \tag{A5}$$

TOV: Transient over-voltages (TOV) at converter bus are an important norm in multi-infeed HVDC. The over-voltages occur because of disturbance in AC or DC network. The severe TOV can arise due to sudden loss of transmitted power of all HVDC systems (in proximity) which reflects surplus amount of reactive power. This phenomenon is called "full load rejection." Full load rejection due to simultaneous blockage of inverters is unlikely. Thus, TOV is mostly occurred due to CFs or faults on AC or DC side. Low MIESCR represents high TOV, which eventually influence ratings of equipment at station and performance of converter. The equation of percentage TOV can be written intuitively as Equation (A6). However, to compute worst case TOV (when all HVDC in proximity are blocked simultaneously), Equation (A7) is used.

$$\%TOV_i = \frac{V_i^N - V_i^{tov}}{V_i^N} \times 100 \tag{A6}$$

Where $V_{\mathrm{i}}^{\mathrm{N}}$ and $V_{\mathrm{i}}^{\mathrm{tov}}$ are voltages at inverter bus *i* during normal and transient over-voltage condition.

$$TOV_i = \sqrt{1.0 + \frac{2 \times Qdc_i}{MIESCR_i} + \frac{1 + Qdc_i^2}{MIESCR_i}} - 1.0 \tag{A7}$$

CFII: Commutation failure (CF) occurs due to abnormalities either on AC or DC side of converter. During CF, converter valve does not transfer current to next valve, which form a short circuit reducing power transfer to zero. The main reason of CF is AC voltage drop (about 20%) due to faults; other reasons include rise in HVDC current and malfunction of control system. Commutation Failure Immunity Index (CFII) is a measure of CF susceptibility, which describes strength of system to withstand maximum fault MVA. The CFII quantifies the immunity of HVDC converter to CF as

$$CFII_i = \frac{(Worst\,Fault\,MVA)_i}{Pdc_i} \times 100 \tag{A8}$$

Here, *Worst Fault MVA* is value of maximum fault, which does not cause CF.